

DMD #32201

Cytochrome P450 1A2 detoxicates aristolochic acid in the mouse.

Thomas A. Rosenquist, Heidi J. Einolf, Kathleen G. Dickman, Lai Wang, Amanda Smith,
Arthur P. Grollman

Laboratory of Chemical Biology, Department of Pharmacological Sciences, Stony Brook University, Stony Brook, NY 11794 (T.A.R., K.G.D.,A.P.G.) and Novartis Institutes of Biomedical Research, One Health Plaza, East Hanover, NJ 07834 (H.J.E., L.W., A.S.).

DMD #32201

Running Title: CYP450 1A2 detoxicates aristolochic acid.

Corresponding Author

Thomas A. Rosenquist

Department of Pharmacological Sciences

State University of New York

One Nicolls Road

Stony Brook, NY 11794-8651

1(631)444-8054 (telephone), 1(631)444-3218 (fax), rosenquist@pharm.stonybrook.edu

Text pages: 27

#Tables: 1

#Figures: 5

References: 31

words in Abstract: 246

#words in Introduction: 646

#words in Discussion: 922

Abbreviations:

AAI, aristolochic acid I, 8-methoxy-6-nitro-phenanthro-(3,4-*d*)-1,3-dioxolo-5-carboxylic acid

AAII aristolochic Acid II, 6-nitro-phenanthro-(3,4-*d*)-1,3-dioxolo-5-carboxylic acid

ALI, aristolactam I

ALII aristolactam II

dA-ALI, 7-(deoxyadenosin-*N*⁶-yl)aristolactam I

dG-ALI, 7-(deoxyguanosine-*N*²-yl)aristolactam I

CYP, cytochromeP450

3MC, 3-metylcholanthrene

DMD #32201

Abstract

Aristolochic acids (AA) are plant-derived nephrotoxins and carcinogens responsible for chronic renal failure and associated urothelial cell cancers in several clinical syndromes known collectively as aristolochic acid nephropathy (AAN). Mice provide a useful model for study of AAN as the renal histopathology of AA-treated mice is strikingly similar to that of humans. AA is also a potent carcinogen in mice with a somewhat different tissue spectrum than in humans. The toxic dose of AA in mice is higher than in humans, this difference in susceptibility has been postulated to reflect differing rates of detoxication between the species. Recent studies in mice have shown that the hepatic cytochrome P450 system detoxicates AA and inducers of the arylhydrocarbon response protect mice from the nephrotoxic effects of AA. The purpose of this study was to determine the role of specific CYP enzymes in AA metabolism *in vivo*. Of eighteen human CYP enzymes we surveyed only two, CYP1A1 and CYP1A2, were effective in de-methylating AAI to the nontoxic derivative AAIA. Kinetic analysis revealed similar efficiencies of formation of AAIA by human and rat CYP1A2. We also report here that CYP1A2-deficient mice display increased sensitivity to the nephrotoxic effects of AAI. Further, *Cyp1a2* knockout mice accumulate AAI-derived DNA adducts in the kidney at a higher rate than control mice. Differences in bioavailability or hepatic metabolism of AAI, expression of CYP1A2, or efficiency of a competing nitroreduction pathway *in vivo* may explain the apparent differences between human and rodent sensitivity to AAI.

DMD #32201

Introduction

Aristolochic acids (AA) are nitrophenanthrene carboxylic acids found in various *Aristolochia* species used as traditional herbal medicines throughout the world (Jameson CW et al., 2008). Chronic exposure to AA is responsible for aristolochic acid nephropathy (AAN) and for Balkan Endemic Nephropathy (BEN) (reviewed in (Grollman et al., 2007; Debelle et al., 2008)). Hallmarks of each disease are proximal tubule atrophy and tubulointerstitial fibrosis leading to end stage renal disease. At least half of these patients also develop cancers of the upper urinary track.

Commercial preparations of AA are composed of mixtures of AAI (8-methoxy-6-nitro-phenanthro-(3,4-*d*)-1,3-dioxolo-5-carboxylic acid) and AAI (6-nitro-phenanthro-(3,4-*d*)-1,3-dioxolo-5-carboxylic acid), compounds that differ only by the presence of an *O*-methoxy group in AAI. AAI is far more cytotoxic than AAI both in simian kidney cells in culture (Balachandran et al., 2005) and in treated animals (Shibutani et al., 2007).

In animals and cell culture, AA is metabolized by several mechanisms. One pathway involves reduction of the nitro group and concomitant condensation with the carboxylic acid moiety to form aristolactam-I (ALI) and aristolactam II (ALII). An intermediate in this pathway, *N*-hydroxyaristolactam, is believed to form a cyclic *N*-acylnitrenium ion that forms adducts with exocyclic amines of purines in DNA. Indeed, the promutagenic 7-(deoxyadenosin-*N*⁶-yl)aristolactams (dA-ALI and dA-ALII) have been observed in the DNA of all species examined after treatment with AA. A:T → T:A transversions, the most frequently observed mutation in the *TP53* gene in urothelial tumors of patients with AAN and BEN (Lord et al., 2004; Grollman et al., 2007), has been proposed to be a “fingerprint” mutation for aristolochic acid exposure (Grollman et al., 2007).

DMD #32201

Furthermore aristolactam metabolites are observed in the urine of various species treated with AA (Krumbiegel et al., 1987). Thus, this pathway is postulated to be universal in mammals.

The second detoxication pathway involves demethylation of AAI to form the nontoxic 8-hydroxy-6-nitro-phenanthro-(3,4-*d*)-1,3-dioxolo-5-carboxylic acid (AA-1a). AAIA and its metabolites have been observed in the urine and feces of rabbits, dogs, mice and rats treated with AAI, but not in urine from humans exposed to AA (Krumbiegel et al., 1987).

A number of defined enzyme systems can activate AA to form DNA adducts *in vitro*.

These include the microsomal enzymes NADPH:CYP reductase (Stiborova et al., 2001c; Stiborova et al., 2005a), prostaglandin H synthase (Stiborova et al., 2001a; Stiborova et al., 2005a) and CYP1A1/2 under anaerobic conditions (Schmeiser et al., 1986; Stiborova et al., 2001b; Stiborova et al., 2005b). Cytoplasmic enzymes implicated in AA-activation include NAD(P)H:quinone oxidoreductase (Stiborova et al., 2002; Stiborova et al., 2003; Stiborova et al., 2005a) and SULT1A1 (Meinl et al., 2006). Under aerobic conditions, hepatic microsomes from rats and humans demethylate AAI to form AAIA (Schmeiser et al., 1986; Sistkova et al., 2008).

Recently, mice deficient in hepatic cytochrome P450 activity were shown to have increased sensitivity to the nephrotoxic effects of AA (Xiao et al., 2008). Conversely, pre-treatment of mice with 3-methylcholanthrene (Xue et al., 2008) or beta-naphthoflavone (Xiao et al., 2009), agonists of the arylhydrocarbon receptor that induce CYP1 enzymes and other xeno-metabolizing activities, protects mice from AA.

The purpose of this study was to delineate the role of specific CYP enzymes *in vivo* in AA-detoxication. We report that CYP1A1 and CYP1A2 are the most active of 18 human

DMD #32201

CYPs tested in demethylating AAI. Kinetic analyses revealed that rat and human CYP1A2 enzymes were similarly efficient in catalyzing the formation of AAIs. However, species differences were found in the efficiency of CYP1A1 vs. CYP1A2 to catalyze the demethylation reaction.

We show also that *Cyp1a2*-null mice are relatively more sensitive to AAI-elicited nephrotoxicity. This increased sensitivity can be reversed by pre-treatment with 3-methylcholanthrene. Additionally, CYP1A2-null mice accumulate ALI-DNA adducts at a higher rate than control mice. Taken together, these results indicate that, in rodents, AAI de-methylation, mediated by CYP1A2, is a primary pathway of AAI detoxication. If the de-methylation pathway is compromised, DNA adducts continued to accumulate indicating that AAI-nitroreduction is increased.

DMD #32201

Methods

Materials and reagents

Reagents -- AAI was purified from a mixture of AA-I and AA-II (40:60) purchased from Fisher Scientific Co. (Fairlawn, NJ) as described (Shibutani et al., 2007). 3-methylcholanthrene was purchased from Sigma-Aldrich (St. Louis, MO). Human and rat recombinant CYP1A1 and CYP1A2 enzymes and pooled human liver microsomes were purchased from BD Biosciences (Woburn, MA). Micrococcal nuclease and potato apyrase were purchased from Sigma-Aldrich (St. Louis, MO), spleen phosphodiesterase from Worthington Biochemical Corp. (Lakewood, NJ) and 3'-phosphatase-free T4 polynucleotide kinase and nuclease P1 from Roche Applied Science (Indianapolis, IN). [γ - 32 P]-ATP (specific activity, >6000 Ci/mmol) was obtained from Amersham Biosciences Corp. (Piscataway, NJ). [3 H]AAI was kindly provided by Tapan Ray, Novartis Institutes of Biomedical Research (East Hanover, NJ). The radiochemical purity of [3 H]AAI was >98% and chemical purity was \geq 93%. Anti-Cyp1A1 rabbit IgG and anti-Cyp1A2 goat IgG and corresponding peroxidase-conjugated secondary antibodies were purchased from Santa Cruz Biotechnology (Santa Cruz, CA). Protein electrophoresis gels, membranes, buffers and electrochemical detection kits were obtained from Thermo Scientific (Rockford, IL.). All other chemical and reagents were purchased from commercial sources.

Urinalysis Kits -- Mouse Albuwell microalbuminuria ELISA kits were purchased from Exocell (Philadelphia, PA). Creatinine Quantichrome assay kits were purchased from BioAssay Systems (Hayward, CA). All urinalysis kits were used following manufacturers instructions.

DMD #32201

Mice -- Animal protocols were reviewed and approved by the Stony Brook IACUC. Breeding pairs of Cyp1A2 knockout mice were obtained from Dr. F. Gonzalez, NCI, NIH. A colony was maintained by breeding in the Stony Brook University animal facility. Control 129S1/SvImJ mice were purchased from Jackson Laboratories (Bar Harbor, Maine). All experiments used 8-week old male mice.

Metabolism of [³H]AAI by human liver microsomes -- For all the *in vitro* metabolism incubations in this report, the buffer components consisted of 100 mM potassium phosphate buffer (pH 7.4) and 5 mM MgCl₂ (final concentrations). For the glucuronidation reactions (containing UDPGA), microsomes were preincubated with alamethicin (60 μg alamethicin·mg protein⁻¹, final concentration) for 15 min on ice prior to addition of MgCl₂ and [³H]AAI. All reactions were pre-incubated at 37°C prior for 3 min prior to co-factor initiation (1 mM NADPH and/or 4 mM UDPGA). Human liver microsomes (1 mg protein·mL⁻¹) were incubated with [³H]AAI (95 μM) and initiated with NADPH and/or UDPGA and were incubated for 30 min at 37°C (final reaction volume of 0.2 mL). Control incubations contained all reaction components without co-factors. Reactions were quenched by the addition of an equal volume of cold acetonitrile and the precipitated protein removed by centrifugation at 39,000 x g for 10 min at ~4°C.

HPLC analysis of [³H]AAI and metabolites -- Samples (25 μL) were analyzed by reversed-phase HPLC on a Waters XTerra MS C₁₈ column (250 x 4.6 mm, 5 μm) at ambient temperature. Gradient elution was achieved using solvent A (0.1 M ammonium acetate, pH 7.5, v/v) and solvent B (acetonitrile) at a flow rate of 1.2 mL·min⁻¹. The HPLC eluate was collected with a fraction collector (FC204 Gilson Inc., Middleton, WI) at 0.2 min per fraction into Deepwell LumaPlate-96 plates (PerkinElmer Life and

DMD #32201

Analytical Sciences). The fractions were dried with a stream of nitrogen and radioactivity was counted with a TopCount NXT Microplate Scintillation and Luminescence Counter (PerkinElmer Life and Analytical Sciences) at a counting time of 10 min per well. Chromatograms from the TopCount were evaluated using IN/US Systems Winflow HPLC application software version 1.4a (IN/US, Tampa, FL) and plotted using SigmaPlot software (SigmaPlot 2002 for Windows, version 8.0, Jandel Corporation, USA).

Metabolism of [³H]AAI by specific human recombinant P450 enzymes -- [³H]AAI (95 mM) was incubated with the recombinant human P450 enzymes: CYP1A1, CYP1A2, CYP1B1, CYP2A6, CYP2B6, CYP2C8, CYP2C9, CYP2C18, CYP2C19, CYP2D6, CYP2E1, CYP2J2, CYP3A4, CYP3A5, CYP4A11, CYP4F2, CYP4F3A, CYP4F3B (100 pmol P450·mL⁻¹) or control P450 microsomes in the presence of NADPH for 30 min at 37°C (final reaction volume of 0.4 mL). The buffer components, sample processing, and HPLC analysis were as described above.

Kinetic analysis of [³H]AAI metabolism by recombinant human or rat CYP1A1 and CYP1A2 -- Steady-state kinetic parameters associated with recombinant human hCYP1A2 and rat (r) rCYP1A2 were determined to establish the efficiency of [³H]AAI metabolism by these enzymes. hCYP1A1 (10 pmol P450·mL⁻¹, 0.11 mg microsomal protein·mL⁻¹), hCYP1A2 (10 pmol P450·mL⁻¹, 0.067 mg microsomal protein·mL⁻¹, final concentration), rCYP1A1 (25 pmol P450·mL⁻¹, 0.0625 mg microsomal protein·mL⁻¹, final concentration), or rCYP1A2 (10 pmol P450·mL⁻¹, 0.05 mg microsomal protein·mL⁻¹, final concentration) were incubated with varying concentrations of [³H]AAI (in duplicate) in the presence of NADPH for 10 min (final reaction volume of 0.2 mL). The

DMD #32201

concentration of CYP enzyme and reaction time was pre-determined to be optimal to ensure \sim <20% turnover of AAI during the incubation. Control samples at each concentration of [^3H]AAI did not contain NADPH. The buffer components, sample processing, and HPLC analysis were as described above. [^3H]AAI metabolism activity was plotted against substrate concentration and the kinetic parameters, K_m and V_{max} , were determined by non-linear regression.

Treatment of mice with aristolochic acid -- Eight-week old male mice were injected intraperitoneally (ip) with 2 mg/kg AAI dissolved in phosphate-buffered saline without divalent cations (Sigma). Several groups of mice were pre-treated the previous day with a single *i.p.* injection of 3-methylcholanthrene (60 mg/kg) in corn oil. This dose of 3MC has previously been shown to induce resistance to AA-nephrotoxicity in mice (Xue et al., 2008). Control animals received vehicle-only injections. For urine collections mice were housed overnight in metabolic cages. Mice were euthanized by CO_2 asphyxiation and tissues collected for microsome and DNA preparation.

Microsomal preparation and protein quantification -- Hepatic microsomes were prepared by homogenization of freshly thawed mouse liver in a Potter S homogenizer (B. Braun Biotech Inc., Allentown, PA) containing microsomal homogenization buffer (0.25 M sucrose, 0.154 M KCl, 0.05 M Tris-HCl, 0.001 M EDTA, 0.25 mM PMSF, pH 7.4) at a concentration of 3 mL buffer per gram of tissue. The homogenate was centrifuged at 10,000 x g for 20 min at 4°C. The supernatant (S9) was transferred to fresh ultracentrifuge tubes and centrifuged at 105,000 x g for 1 h at 4°C. The top lipid layer and cytosol was aspirated and the microsomal pellet was resuspended in storage buffer (0.1 M potassium phosphate buffer, pH 7.4, 20% glycerol, v/v) at an estimated final

DMD #32201

concentration of 1 mL storage buffer per gram tissue (starting amount) using a dounce homogenizer. Aliquots of approximately 50 μ L each were stored at -80°C . The amount of microsomal protein was determined by the Bradford protein assay method.

Metabolism of [^3H]AAI in mouse liver microsomes -- The metabolism of [^3H]AAI was examined in mouse liver microsomes prepared from control or 3-MC treated wild-type or *cyp1a2*^{-/-} mice. Mouse liver microsomes (1 mg protein·mL⁻¹) were preincubated with alamethicin, as described above, prior to incubation with [^3H]AAI (95 μM , final concentration). The reactions were initiated with UDPGA and NADPH and the samples incubated for 30 min at 37°C . Control incubations contained all reaction components without co-factors. The buffer components, sample processing, and HPLC analysis were as described above.

Extraction and digestion of renal cortical DNA -- DNA was extracted from cortical slices from freshly isolated kidneys using a Qiagen DNeasy Blood and Tissue kit (Valencia, CA) according to the manufacturer's protocol. The concentration of DNA was determined by UV spectroscopy. One microgram of DNA was digested enzymatically at 37°C for 16 hours in 100 μl of 17 mM sodium succinate buffer (pH 6.0) containing 8 mM CaCl_2 , micrococcal nuclease (30 units) and spleen phosphodiesterase (0.15 unit) (32). The reaction mixture was incubated for one hour with nuclease P1 (1 unit), whereupon 200 μl of water was added. The reaction samples then were extracted twice with 200 μl of butanol; the butanol fractions were combined, back-extracted with 50 μl of distilled water and evaporated to dryness.

^{32}P -Postlabeling/polyacrylamide-gel electrophoresis (PAGE) analysis -- DNA digestion mixtures were incubated at 37°C for 40 min with 10 mCi of [γ - ^{32}P]-ATP and

DMD #32201

3'-phosphatase-free T4 polynucleotide kinase (10 units), followed by incubation with apyrase (50 milliunits) for 30 min, as described previously (32). The ^{32}P -labeled products were separated by electrophoresis for 4-5 hours on a nondenaturing 30% polyacrylamide gel (35 x 42 x 0.04 cm) with 1500-1800 V/20-40 mA. The position of ^{32}P -labeled adducts was established by β -phosphorimager analysis (Molecular Dynamics Inc.). To quantify the ^{32}P -labeled products, integrated values were measured using a β -phosphorimager and compared with the standards. As ALI_DNA adducts were not available, a known amount (0.0152pmol) of dA-ALII or dG-ALII-modified oligodeoxynucleotides were used as standards (obtained from Francis Johnson, Department of Chemistry, Stonybrook University) (Attaluri et al., 2009).

Immunoblotting microsomal proteins -- Fifty micrograms of each microsomal protein preparation were subjected to electrophoresis through a 4-20% gradient SDS-polyacrylamide gel (Thermo Scientific, Rockford, IL.) then electro-transferred to a nitrocellulose membrane (Thermo Scientific, Rockford, IL.). Membranes were pre-blocked with 5% milk protein in TBST (150 mM sodium chloride, 50 mM Tris, pH 7.5, 0.2% Tween-20 detergent), then incubated at room temperature with primary antibody, at 0.2 micrograms per ml, in blocking buffer for two hours followed by washing in TBST. Secondary antibody was diluted (1:20,000) in blocking buffer and incubated with the membrane for one hour followed by washing in TBST. Antibody was detected with electrochemical reagents and film exposure following manufacturer's protocols (Thermo Scientific, Rockford, IL.).

DMD #32201

Results

Figure 1 shows the current model of AAI metabolism in mammals. Two pathways are envisioned; intermediates in either pathway may be substrates for the other. AAI can be directly de-methylated to form AAIA, as shown in the upper arm of the figure. AAIA is relatively non-toxic in kidney cells in culture (Balachandran et al., 2005) and in mice (Shibutani et al., 2010). AAI undergoes nitro-reduction to ALL, as shown in the lower arm of the pathway (Fig 1). Activated intermediates in this pathway form covalent adducts with DNA and proteins. The end products are conjugated to glucuronic acid or sulfate by phase II enzymes, enhancing solubility and promoting excretion.

As shown in Figure 2A, [³H]AAI is metabolized by human liver microsomes in the presence of NADPH by de-methylation to form AAIA. In the presence of UDPGA, a glucuronidation product was found with an elution time of ~27 min under these chromatographic conditions. The identification of AAIA and the glucuronidation product in the human liver microsomes samples were confirmed by LC/MS/MS (data not shown). We examined eighteen individual human cytochrome P450 enzymes for their ability to metabolize AAI. AAIA was formed primarily by CYP1A2 and CYP1A1 (Figure 2B). With the exception of marginal CYP2C9 activity, no other human CYP tested was active in this assay. Due to negligible expression of CYP1A1 in un-induced human liver, it is likely that CYP1A2 predominates in the formation of this metabolite in human liver. Kinetic parameters associated with metabolism of [³H]AAI, catalyzed by human or rat recombinant CYP1A1 and CYP1A2 enzymes, are summarized in Table 1. Rat and human CYP1A2 enzymes were equally efficient in demethylating AAI (V_{max}/K_m values of 43.2 and 31.6 mL·h⁻¹·nmol P450⁻¹, respectively). Species differences were found, however,

DMD #32201

for CYP1A1. Thus, formation of AA1a catalyzed by rat CYP1A1 was 126-fold lower than rat CYP1A2, whereas human CYP1A1 was ~4-fold more efficient than human CYP1A2 in producing this metabolite.

To determine if CYP1A2 is required *in vivo* for metabolism of AAI in mice we treated *Cyp1a2*^{-/-} and *Cyp1a2*^{+/+} control mice with a single, moderate dose (2.0 mg/kg) of AAI. Urine was collected during the week following treatment and analyzed for albumin and creatinine content. The toxin induces proximal tubule cell toxicity manifested by reduced re-uptake of low molecular weight proteins in the proximal nephron and the presence of injury markers in the urine (Huang et al., 2009). Four days after AAI-treatment, there is an increase in the amount of urinary albumin, as shown in Fig. 3. As proximal tubule function is restored, albuminuria decreases and eventually disappears. The urine of AAI-treated *Cyp1a2*^{-/-} mice contained higher levels of albumin and for a longer period of time, than *Cyp1a2*^{+/+} control mice, indicating a higher degree of nephrotoxicity for AAI in CYP1A2-deficient mice.

3-methylcholanthrene (3MC) induces several biotransformation activities, including CYP1A, and pre-treatment of mice with 3MC is reported to increase resistance to AAI-elicited nephrotoxicity (Xue et al., 2008). We pre-treated *Cyp1a2*^{-/-} or control mice with 60 mg/kg 3MC or vehicle and 24 hours later treated them with AAI as in the previous experiment. Both 3MC-pretreated control and *Cyp1a2*^{-/-} mice displayed increased resistance to AAI relative to non-induced mice (Figure 3). AAI-dependent albuminuria in the induced *Cyp1a2*^{-/-} mice was equivalent to that of un-induced control mice.

To assess the AAI-metabolizing activities in *Cyp1a2*^{-/-} mice, we isolated hepatic microsomes from knockout and control mice both with and without pre-treatment with

DMD #32201

3MC. These microsomes were utilized in the AAI assay described above and results are shown in Figure 4A and 4B. Microsomes from control mice produce primarily AAIA, the level of which is increased by pre-treatment with 3MC. Microsomes from *Cyp1a2*^{-/-} mice produced little AAIA, providing confirmatory evidence that CYP1A2 is the primary hepatic enzyme responsible for demethylating AAI. Microsomes from 3MC-treated *Cyp1a2*^{-/-} mice produce increased AAIA indicating the induction of another CYP-activity (most likely CYP1A1 (*vide infra*). Several unidentified metabolites (indicated by peaks numbered 1, 2, and 3 in Figure 4B) also are produced.

3MC is known to induce the expression of CYP1A1 and CYP1A2 and, in Figure 4C, we show that in the *Cyp1a2*^{-/-} mice CYP1A1 protein was indeed induced in the liver. In *Cyp1a2*^{+/+} mice, we observed induction of CYP1A2 but not CYP1A1 under these conditions. The increase of CYP1A2 is consistent with the elevated AAIA levels observed and increased resistance of these mice to AAI relative to un-induced mice.

We hypothesize that animals unable to detoxicate AAI thru demethylation would be more susceptible to formation of aristolactam-I-DNA adducts (ALI-dG and ALI-dA) that are a side-product of nitroreduction of AAI, the second pathway contributing to AAI metabolism. To assess this reaction, we isolated kidney cortex DNA from mice euthanized 4 hours and 20 hours after treatment with AAI and measured ALI-DNA adducts by the ³²P-post-labelling technique. As shown in Figure 5A and 5B, the *Cyp1a2*^{-/-} mice, deficient for AAI-demethylating activity, accumulate higher levels of ALI-DNA adducts.

DMD #32201

Discussion

The ability to demethylate AAI may determine the toxic potential of AA in mammalian species. In this paper we establish that CYP1A2 is the major enzyme responsible for demethylation of AAI in mice. We report the most extensive survey of CYP enzymes for AAI-metabolizing activities to date, and the first kinetic analysis of the capabilities of the CYP1A enzymes with respect to AAI-demethylation. Human and rodent CYP1A2 are kinetically similar with respect to this important reaction. If expressed, human hepatic CYP1A1 is also kinetically competent to contribute to detoxication of AAI.

In vitro studies have established that AAI may be metabolized by nitroreduction to ALI and/or demethylation to AAIA (reviewed in (Stiborova et al., 2008)). Aristolactams are formed by several cellular enzymes, including NADPH:CYP reductase, prostaglandin H synthase, and NAD(P)H:quinone oxidoreductase (NQO1). Microsomal AA-metabolism, particularly reactions catalyzed by CYP1A enzymes under anaerobic conditions also lead to the formation of genotoxic intermediates (Schmeiser et al., 1997; Stiborova et al., 2001b; Stiborova et al., 2005a; Stiborova et al., 2005b). Under aerobic conditions, formation of aristolactam-DNA adducts in reactions catalyzed by hepatic microsomes was greatly reduced (Schmeiser et al., 1997) and AAIA was formed (Sistkova et al., 2008). We confirm that under aerobic conditions microsomal CYP1A enzymes demethylate AAI to form AAIA and show they are kinetically competent to do so *in vivo*. AAIA is non-toxic in cells (Balachandran et al., 2005; Shibutani et al., 2010) and even in the presence of reducing agents, is incapable of forming covalent adducts with DNA (Shibutani et al., 2010).

DMD #32201

We report here that among eighteen human cytochrome P450 enzymes tested, only the CYP1A1 and CYP1A2 enzymes have robust AAI demethylating activity. The only other CYP with detectable activity against AAI was CYP2C9. Under homeostatic conditions CYP1A2 is the major CYP1A enzyme expressed in livers of humans and mice ((Gonzalez et al., 1984; Ikeya et al., 1989). Consistent with these observations, we detected little AAI demethylation activity in hepatic microsomes prepared from CYP1A2-null mice. In a pilot genetic study, a weak association between the human CYP3A5*1 allele and Balkan endemic nephropathy, a disease resulting from chronic dietary exposure to AA (Grollman et al, 2007), was noted (Atanasova et al., 2005). However we did not detect AAI-demethylation activity by CYP3A5.

Mice lacking hepatic CYP activity are extremely sensitive to AA, indicating that AA-metabolism occurs primarily in the liver (Xiao et al., 2008). Consistent with this report, AAIA was not detected in renal microsomes (data not shown). Induction of CYP1A activity with 3-MC (Xue et al., 2008) or beta-naphthoflavone (Xiao et al., 2009) increases resistance to AAI-elicited nephrotoxicity. In this study, 3MC treatment increased hepatic microsomal AAI-demethylation activity in both control and CYP1A2-null mice. However, in *Cyp1a2*^{+/+} mice 3MC treatment increased the hepatic expression of CYP1A2 and also increased AAIA formation. In *Cyp1a2*^{-/-} mice we observed induction of CYP1A1 expression. In addition to increased AAIA production, hepatic microsomes from 3MC-induced *Cyp1a2*^{-/-} mice also produced several, as yet unidentified, metabolites of AAI. We speculate that these metabolites include AAIA phase II conjugation products. Thus in the absence of CYP1A2, different activities are induced by 3MC, suggesting the presence of additional enzymes that metabolize AAI.

DMD #32201

We tested *Cyp1a2* knockout mice for their sensitivity to AAI. Microalbuminuria, an indicator of renal proximal tubule dysfunction was elevated after AAI treatment in CYP1A2 deficient mice. Thus, CYP1A2 does plays an important role in detoxication of AAI in mice.

According to the current model of AAI metabolism, reduction in AAI-demethylation activity is expected to increase production of aristolactam metabolites and associated toxicity resulting from ALI-DNA and protein adducts. As predicted, we observed greater accumulation of ALI-DNA adducts in the renal cortex of *Cyp1a2*^{-/-} mice relative to wild type mice. This result is consistent with the proposed model of AAI metabolism. In humans, at least 50% of patients with AA-associated nephropathies develop urothelial carcinomas of the upper urinary tract, characterized by a predominance of A:T->T:A transversions in the TRP53 gene (Grollman et al, 2007. This is in sharp contrast to sporadic urothelial cancers where A:T->T:A transversions are rare (Olivier et al., 2002). To date, AA carcinogenicity has been investigated only in the NMRI strain of mice (Mengs, 1988). In these mice, AA induces primarily cancer of the fore-stomach, and a lower frequency of other tumors including renal adenomas. Our results indicate that the level of ALI-DNA adducts increase significantly in the renal-urothelial system of *Cyp1a2*^{-/-} mice, It will be interesting to determine if CYP1A2 deficiency increases the rate of urothelial cell carcinogenesis in mice.

Both AAI and AAII induce aristolactam DNA adducts (Schmeiser et al., 1988; Shibutani et al., 2007) but AAII is relatively non-toxic to renal cells *in vitro* (Balachandran et al., 2005) and *in vivo* (Shibutani et al., 2007). Thus, AA-induced DNA damage is unlikely to be responsible for the profound toxicity observed in renal proximal tubule cells. It has

DMD #32201

yet to be established if the cytotoxic compound involved is AAI itself or a metabolite.

Reduction of AAI demethylation in *Cyp1a2*^{-/-} mice can have the effect of increasing either.

Finally, it has been noted that urine from AA-exposed humans contains metabolites of aristolactam but not those derived from AAIa (Krumbiegel et al., 1987). This implies that the nitroreduction pathway is more efficient than demethylation in metabolizing AAI in humans. However our results indicate that human CYP1A2 is kinetically similar to rodent CYP1A2 with respect to AAI-demethylation activity. Thus some other aspect of AAI metabolism, perhaps hepatic bioavailability, CYP1A2 expression levels, or increased activity of nitroreductases, underlies the differential susceptibility to AAI between humans and rodents.

DMD #32201

Acknowledgements We are indebted to the expert technical assistance of Penelope Strockbine and a gift of AAI-modified oligonucleotides from Francis Johnson, Stony Brook University.

DMD #32201

References

- Atanasova SY, von Ahsen N, Toncheva DI, Dimitrov TG, Oellerich M and Armstrong VW (2005) Genetic polymorphisms of cytochrome P450 among patients with Balkan endemic nephropathy (BEN). *Clin Biochem* **38**:223-228.
- Attaluri S, Bonala RR, Yang IY, Lukin MA, Wen Y, Grollman AP, Moriya M, Iden CR and Johnson F (2009) DNA adducts of aristolochic acid II: total synthesis and site-specific mutagenesis studies in mammalian cells. *Nucleic Acids Res.*
- Balachandran P, Wei F, Lin RC, Khan IA and Pasco DS (2005) Structure activity relationships of aristolochic acid analogues: toxicity in cultured renal epithelial cells. *Kidney Int* **67**:1797-1805.
- Debelle FD, Vanherweghem JL and Nortier JL (2008) Aristolochic acid nephropathy: a worldwide problem. *Kidney Int* **74**:158-169.
- Gonzalez FJ, Tukey RH and Nebert DW (1984) Structural gene products of the Ah locus. Transcriptional regulation of cytochrome P1-450 and P3-450 mRNA levels by 3-methylcholanthrene. *Mol Pharmacol* **26**:117-121.
- Grollman AP, Shibutani S, Moriya M, Miller F, Wu L, Moll U, Suzuki N, Fernandes A, Rosenquist T, Medverec Z, Jakovina K, Brdar B, Slade N, Turesky RJ, Goodenough AK, Rieger R, Vukelic M and Jelakovic B (2007) Aristolochic acid and the etiology of endemic (Balkan) nephropathy. *Proc Natl Acad Sci U S A* **104**:12129-12134.
- Huang F, Clifton J, Yang X, Rosenquist T, Hixson D, Kovac S and Josic D (2009) SELDI-TOF as a method for biomarker discovery in the urine of aristolochic-acid-treated mice. *Electrophoresis* **30**:1168-1174.
- Ikeya K, Jaiswal AK, Owens RA, Jones JE, Nebert DW and Kimura S (1989) Human CYP1A2: sequence, gene structure, comparison with the mouse and rat orthologous gene, and differences in liver 1A2 mRNA expression. *Mol Endocrinol* **3**:1399-1408.
- Jameson CW, Lunn R, Jeter S, Garner S, Atwood S, Carter G, Levy D and J.-P. C (2008) Background document for aristolochic acid-related exposures, National Toxicology Program Report on Carcinogens. **12th edition**:1-228.
- Krumbiegel G, Hallensleben J, Mennicke WH, Rittmann N and Roth HJ (1987) Studies on the metabolism of aristolochic acids I and II. *Xenobiotica* **17**:981-991.
- Lord GM, Hollstein M, Arlt VM, Roufosse C, Pusey CD, Cook T and Schmeiser HH (2004) DNA adducts and p53 mutations in a patient with aristolochic acid-associated nephropathy. *Am J Kidney Dis* **43**:e11-17.
- Meinl W, Pabel U, Osterloh-Quiroz M, Hengstler JG and Glatt H (2006) Human sulphotransferases are involved in the activation of aristolochic acids and are expressed in renal target tissue. *Int J Cancer* **118**:1090-1097.
- Mengs U (1988) Tumour induction in mice following exposure to aristolochic acid. *Arch Toxicol* **61**:504-505.
- Olivier M, Eeles R, Hollstein M, Khan MA, Harris CC and Hainaut P (2002) The IARC TP53 database: new online mutation analysis and recommendations to users. *Hum Mutat* **19**:607-614.
- Schmeiser HH, Frei E, Wiessler M and Stiborova M (1997) Comparison of DNA adduct formation by aristolochic acids in various in vitro activation systems by 32P-post-

DMD #32201

- labelling: evidence for reductive activation by peroxidases. *Carcinogenesis* **18**:1055-1062.
- Schmeiser HH, Pool BL and Wiessler M (1986) Identification and mutagenicity of metabolites of aristolochic acid formed by rat liver. *Carcinogenesis* **7**:59-63.
- Schmeiser HH, Schoepe KB and Wiessler M (1988) DNA adduct formation of aristolochic acid I and II in vitro and in vivo. *Carcinogenesis* **9**:297-303.
- Shibutani S, Bonala RR, Rosenquist T, Rieger R, Suzuki N, Johnson F, Miller F and Grollman AP (2010) Detoxification of Aristolochic Acid I by O-Demethylation; Less Nephrotoxicity and Genotoxicity of Aristolochic Acid Ia in Rodents *Int J Cancer* **in press**.
- Shibutani S, Dong H, Suzuki N, Ueda S, Miller F and Grollman AP (2007) Selective toxicity of aristolochic acids I and II. *Drug Metab Dispos* **35**:1217-1222.
- Sistkova J, Hudecek J, Hodek P, Frei E, Schmeiser HH and Stiborova M (2008) Human cytochromes P450 1A1 and 1A2 participate in detoxication of carcinogenic aristolochic acid. *Neuro Endocrinol Lett* **29**:733-737.
- Stiborova M, Frei E, Arlt VM and Schmeiser HH (2008) Metabolic activation of carcinogenic aristolochic acid, a risk factor for Balkan endemic nephropathy. *Mutat Res* **658**:55-67.
- Stiborova M, Frei E, Breuer A, Wiessler M and Schmeiser HH (2001a) Evidence for reductive activation of carcinogenic aristolochic acids by prostaglandin H synthase -- (32)P-postlabeling analysis of DNA adduct formation. *Mutat Res* **493**:149-160.
- Stiborova M, Frei E, Hodek P, Wiessler M and Schmeiser HH (2005a) Human hepatic and renal microsomes, cytochromes P450 1A1/2, NADPH:cytochrome P450 reductase and prostaglandin H synthase mediate the formation of aristolochic acid-DNA adducts found in patients with urothelial cancer. *Int J Cancer* **113**:189-197.
- Stiborova M, Frei E, Sopko B, Sopkova K, Markova V, Lankova M, Kumstyrova T, Wiessler M and Schmeiser HH (2003) Human cytosolic enzymes involved in the metabolic activation of carcinogenic aristolochic acid: evidence for reductive activation by human NAD(P)H:quinone oxidoreductase. *Carcinogenesis* **24**:1695-1703.
- Stiborova M, Frei E, Sopko B, Wiessler M and Schmeiser HH (2002) Carcinogenic aristolochic acids upon activation by DT-diaphorase form adducts found in DNA of patients with Chinese herbs nephropathy. *Carcinogenesis* **23**:617-625.
- Stiborova M, Frei E, Wiessler M and Schmeiser HH (2001b) Human enzymes involved in the metabolic activation of carcinogenic aristolochic acids: evidence for reductive activation by cytochromes P450 1A1 and 1A2. *Chem Res Toxicol* **14**:1128-1137.
- Stiborova M, Hajek M, Frei E and Schmeiser HH (2001c) Carcinogenic and nephrotoxic alkaloids aristolochic acids upon activation by NADPH : cytochrome P450 reductase form adducts found in DNA of patients with Chinese herbs nephropathy. *Gen Physiol Biophys* **20**:375-392.
- Stiborova M, Sopko B, Hodek P, Frei E, Schmeiser HH and Hudecek J (2005b) The binding of aristolochic acid I to the active site of human cytochromes P450 1A1

DMD #32201

- and 1A2 explains their potential to reductively activate this human carcinogen. *Cancer Lett* **229**:193-204.
- Xiao Y, Ge M, Xue X, Wang C, Wang H, Wu X, Li L, Liu L, Qi X, Zhang Y, Li Y, Luo H, Xie T, Gu J and Ren J (2008) Hepatic cytochrome P450s metabolize aristolochic acid and reduce its kidney toxicity. *Kidney Int* **73**:1231-1239.
- Xiao Y, Xue X, Wu YF, Xin GZ, Qian Y, Xie TP, Gong LK and Ren J (2009) beta-Naphthoflavone protects mice from aristolochic acid-I-induced acute kidney injury in a CYP1A dependent mechanism. *Acta Pharmacol Sin* **30**:1559-1565.
- Xue X, Xiao Y, Zhu H, Wang H, Liu Y, Xie T and Ren J (2008) Induction of P450 1A by 3-methylcholanthrene protects mice from aristolochic acid-I-induced acute renal injury. *Nephrol Dial Transplant* **23**:3074-3081.

DMD #32201

Footnotes

This work was supported by the National Institute of Environmental Health Sciences
[Grant ES04068].

DMD #32201

Figure Legends

Fig. 1. A) Pathways for AAI metabolism in mammals. AAI is demethylated to form AAIA in a reaction catalyzed by cytochrome P450 (CYP). Subsequent conjugation to glucuronic acid or sulfate, catalyzed by UDP glucuronyl transferases (UGT) or sulfotransferases (ST) enhances excretion. Cellular nitroreductases (NR) catalyze formation of the biologically inactive aristolactam (ALI). A reactive intermediate in this pathway, possibly *N*-OH-ALI forms covalent adducts with DNA and proteins. B) Structures of AAI-derived DNA adducts; ALI-dA (7-(deoxyadenosine-*N*⁶-yl)aristolactam I) and ALI-dG (7-(deoxyguanosine-*N*²-yl)aristolactam I). * Position of ³H in radiolabeled AAI used in this study.

Fig. 2. Metabolism of AAI by human CYPs A) [³H]AAI was incubated with human liver microsomes (HLM). Reaction products were separated by HPLC and the radioactivity in each fraction determined. Peaks corresponding to AAIA and AAI-glucuronide are indicated. B) Recombinant human CYP enzymes were tested for their ability to metabolize AAI. Shown is the production of AAIA from AAI by human CYP1A1 and CYP1A2.

Fig. 3. Nephrotoxic effects of AAI in mice. Mice lacking CYP1A2 (*Cyp1a2*^{-/-}) or control mice from the isogenic 129S1/SvImJ strain (*Cyp1a2*^{+/+}) were injected intraperitoneally on day zero with AAI (2 mg/kg); urine was collected at the times indicated and albumin and creatinine levels were measured. The mice were injected with 3-MC (60 mg/kg) or corn oil (-3MC) 24 hours prior to treatment with AAI. All data represent averages of two mice (error bar=SEM). Urinary albumin levels in untreated mice of both strains is <0.1 mg per mg of creatinine.

DMD #32201

Fig 4. Metabolism of AAI by hepatic microsomes from *Cyp1a2*^{-/-} mice. Microsomes isolated from livers of *Cyp1a2*^{+/+} or *Cyp1a2*^{-/-} mice were incubated with [³H]AAI as described in Methods. Products were analyzed by HPLC with off-line low level radioactivity detection. Panel A shows products produced by microsomes from un-induced mice. Panel B shows products produced by microsomes from mice pre-treated with 3MC 24 hours prior to treatment with AAI. . Peaks corresponding to AAI and AAIs are indicated. Peaks 1,2, and 3 are unidentified products. Each result was reproduced in two mice. Panel C shows immunoblots of hepatic microsomal protein from two mice obtained from each treatment described above and reacted with antibodies to CYP1A2 (α -CYP1A2) or CYP1A1 (α -CYP1A1). Arrowhead indicates Cyp1A1.

Fig 5 Increase of ALI-DNA adducts in mice lacking CYP1A2. Genomic DNA was isolated from the renal cortex four and 20 hours after treatment with AAI (2 mg/kg). ³²P-postlabelling analysis was performed as described in Methods. A) ³²P ALI-DNA adducts in renal cortex of three *Cyp1a2*^{-/-} mice (lanes 2-4) and three *Cyp1a2*^{+/+} mice (lanes 5-7) analyzed 20 hours following treatment with AAI. Standards (S) in lane 1 were ALII-dG and ALII-dA. ALII-nucleosides are 30 daltons less than ALI-nucleosides and migrate slightly faster than ALI adducts (indicated by ALI-dG and ALI-dA) under the conditions employed here. B) Radioactivity in each band from the experiment shown in panel A, and a similar experiment with a four hour time point, was determined by phospho-imager and the concentration of ALI-dG and ALI-dA established by comparison to the standards. The concentrations of the pro-mutagenic ALI-dA DNA adduct from either *Cyp1a2*^{+/+} or *Cyp1a2*^{-/-} mice is shown. N=3. ** p<0.01, Student's one-tailed t-test.

DMD #32201

Table 1. Kinetic parameters of human and rat CYP1A1 and CYP1A2 for AAI metabolism

	K_m	V_{max}	V_{max}/K_m
	(μM)	($nmol \cdot h^{-1} \cdot nmol P450^{-1}$)	($mL \cdot h^{-1} \cdot nmol P450^{-1}$)
Human CYP1A1	19.7 ± 5.9	2330 ± 236	118
Human CYP1A2	53.6 ± 15.0	1692 ± 256	31.6
Rat CYP1A1	659 ± 247	227 ± 111	0.344
Rat CYP1A2	12.0 ± 5.0	523 ± 62	43.2

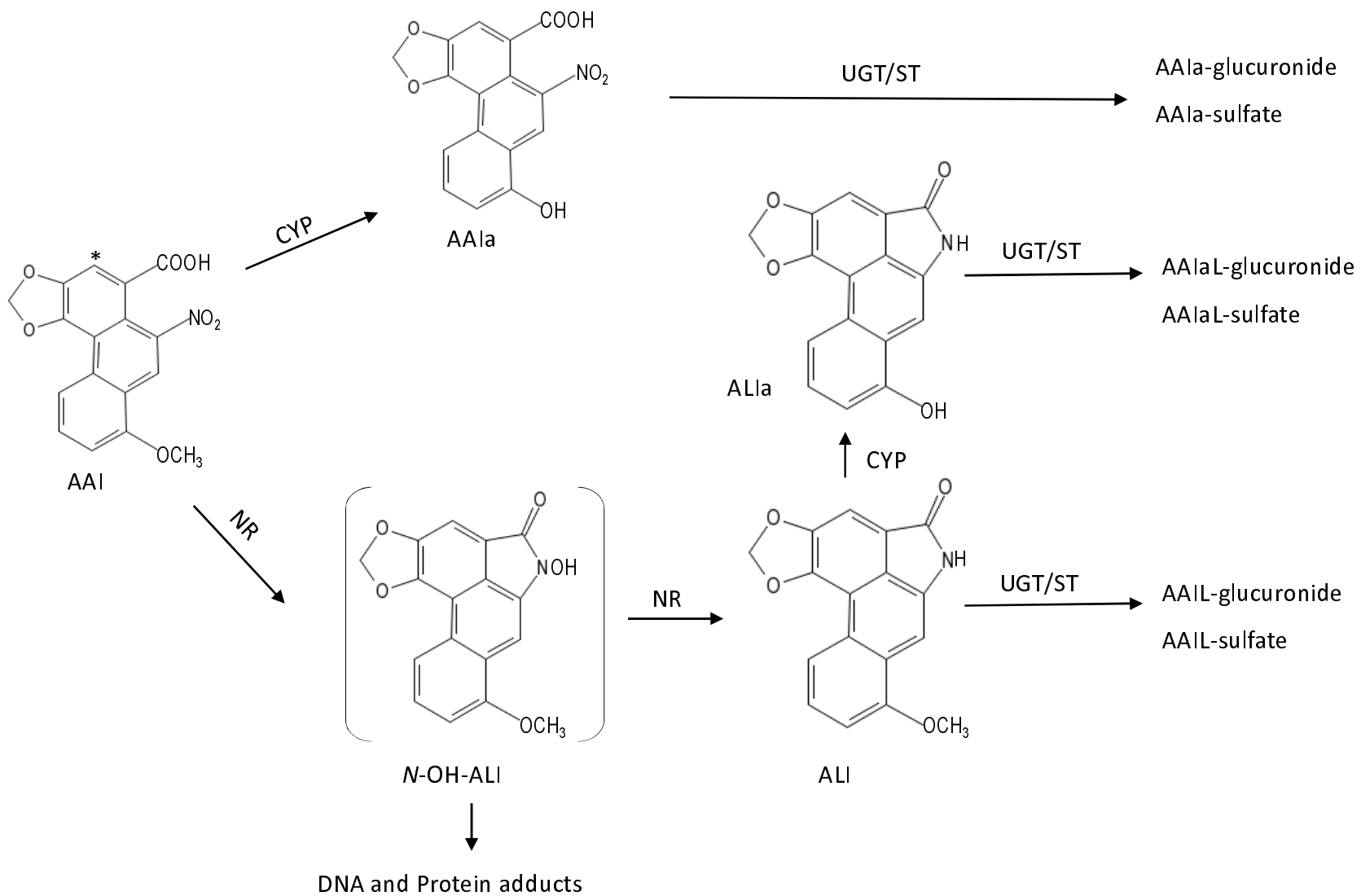
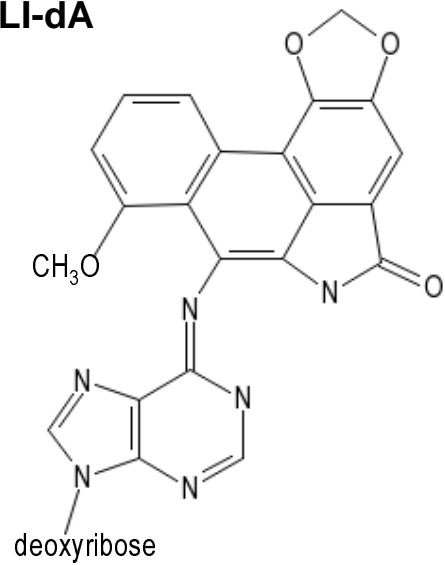


Figure 1A

ALI-dA



ALI-dG

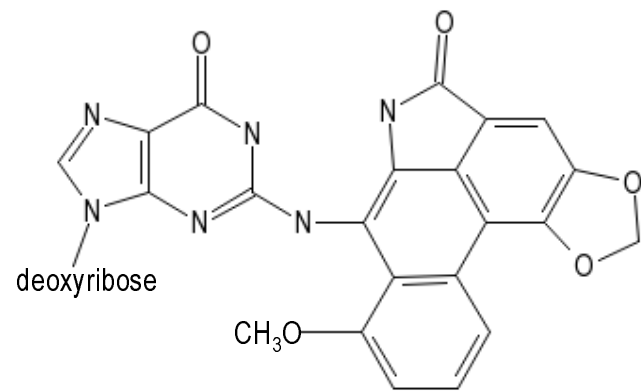


Figure 1B

Figure 2

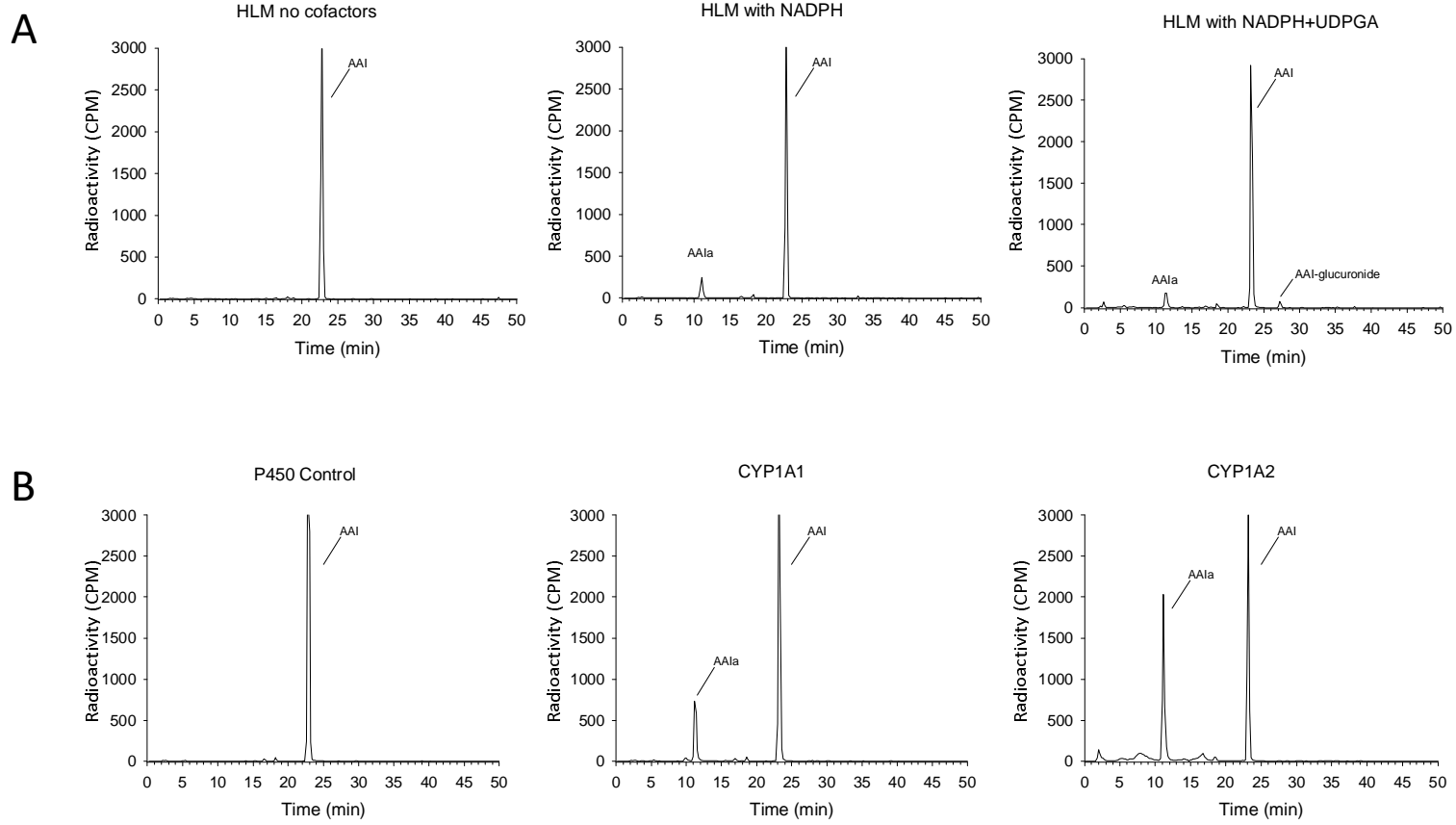
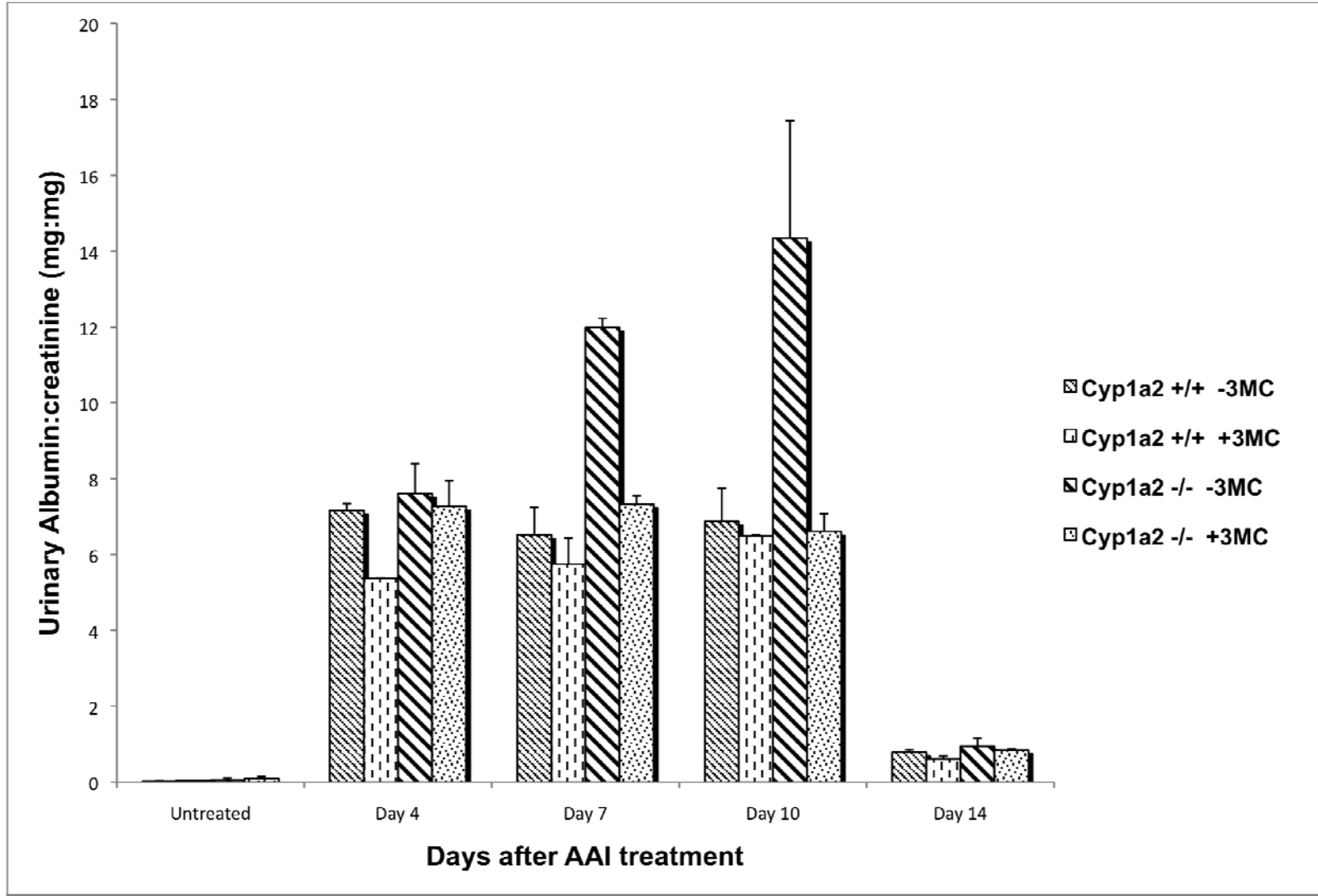


Figure 3



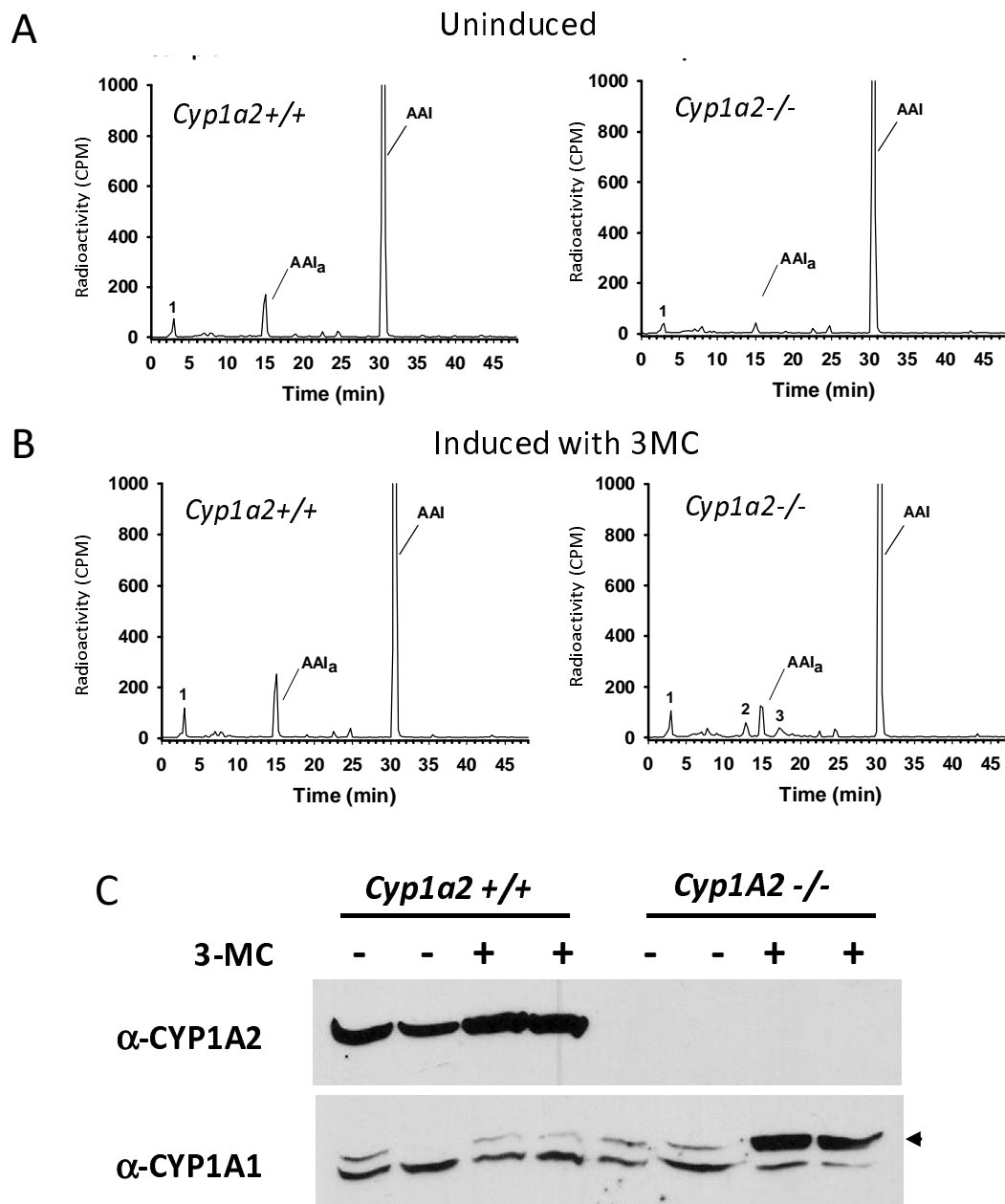


Figure 4

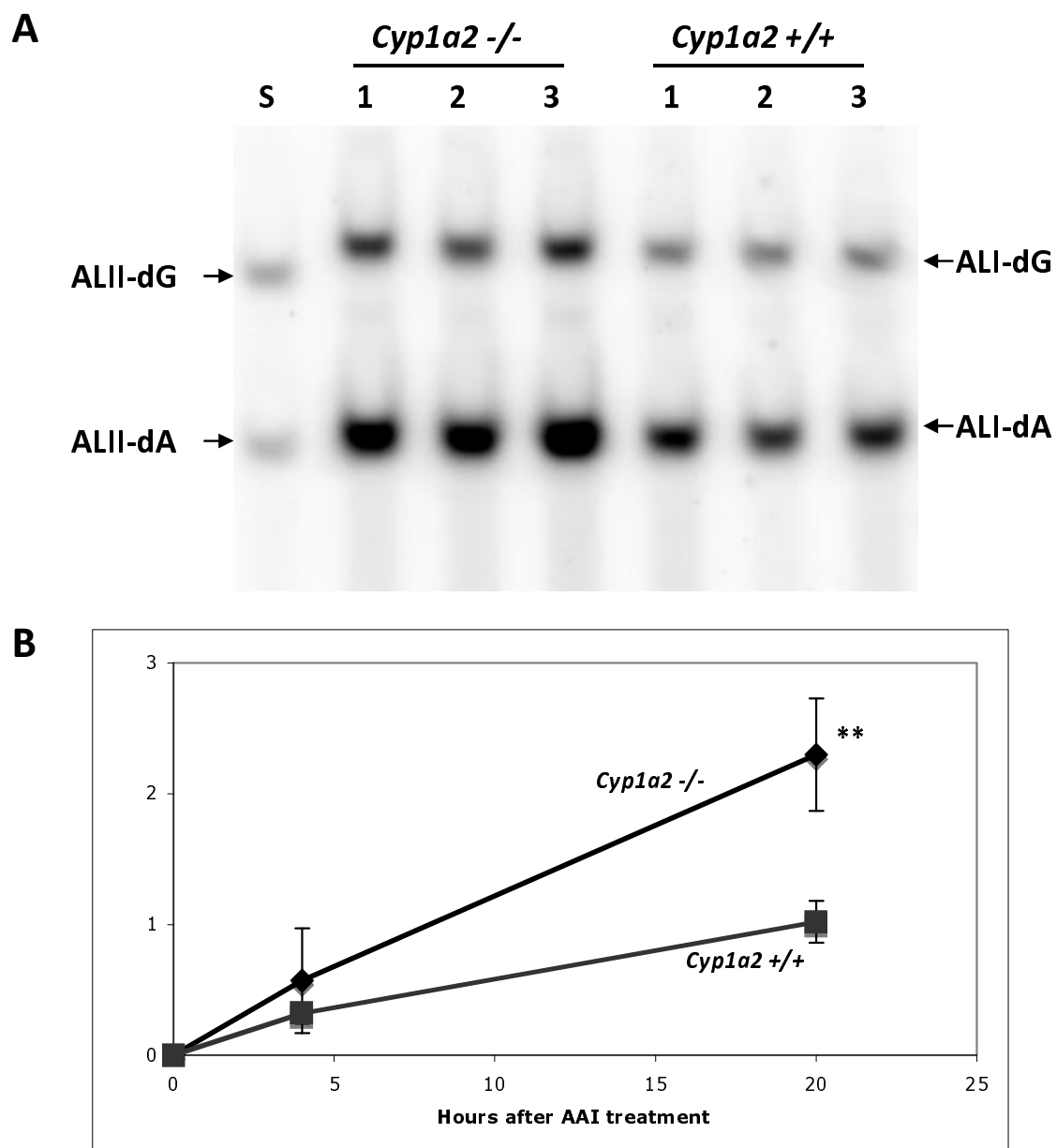


Figure 5